Available online at www.sciencedirect.com
SCIENCE DIRECT
ELSEVIER
Icarus 183 (2006) 403–410
ICARUS
www.elsevier.com/locate/icarus

Subvisible CO_2 ice clouds detected in the mesosphere of Mars

Franck Montmessin [a,*], Jean-Loup Bertaux [a], Eric Quémerais [a], Oleg Korablev [b], Pascal Rannou [a], François Forget [c], Séverine Perrier [a], Didier Fussen [d], Sébastien Lebonnois [c], Aurélie Rébérac [a], Emmanuel Dimarellis [a]

[a] *Service d'Aéronomie, CNRS/UVSQ/IPSL, Réduit de Verrières, Route des Gatines, 91371 Verrières-le-Buisson Cédex, France*
[b] *Space Research Institute (IKI), 84/32 Profsoyuznaya, 117810 Moscow, Russia*
[c] *Laboratoire de Météorologie Dynamique, CNRS/UPMC/IPSL, Paris, France*
[d] *Belgian Institute for Space Aeronomy, 3 ave. Circulaire, B-1180 Brussels, Belgium*

Received 3 November 2005; revised 28 March 2006

Available online 5 June 2006

Abstract

The formation of CO_2 ice clouds in the upper atmosphere of Mars has been suggested in the past on the basis of a few temperature profiles exhibiting portions colder than CO_2 frost point. However, the corresponding clouds were never observed. In this paper, we discuss the detection of the highest clouds ever observed on Mars by the SPICAM ultraviolet spectrometer on board Mars Express spacecraft. Analyzing stellar occultations, we detected several mesospheric detached layers at about 100 km in the southern winter subtropical latitudes, and found that clouds formed where simultaneous temperature measurements indicated that CO_2 was highly supersaturated and probably condensing. Further analysis of the spectra reveals a cloud opacity in the subvisible range and ice crystals smaller than 100 nm in radius. These layers are therefore similar in nature as the noctilucent clouds which appear on Earth in the polar mesosphere. We interpret these phenomena as CO_2 ice clouds forming inside supersaturated pockets of air created by upward propagating thermal waves. This detection of clouds in such an ultrararefied and supercold atmosphere raises important questions about the martian middle-atmosphere dynamics and microphysics. In particular, the presence of condensates at such high altitudes begs the question of the origin of the condensation nuclei.

Keywords: Mars, atmosphere; Occultations

1. Introduction

One of the most interesting meteorological phenomena of the Solar System is believed to occur during the formation of a particular type of cloud on Mars. The main constituent of the atmosphere (carbon dioxide accounts for 95% of the air mass) is suspected indeed to condense onto itself, in addition to its direct deposition as frost on the surface of mid-to-high latitudes in fall and winter. Many independent, although inconclusive, observations provide strong contention for the existence of CO_2 ice clouds in the martian polar nights. There, atmospheric temperature has been observed to fall below that at which CO_2 should condense (Hinson and Wilson, 2002). Additionally, lidar echoes obtained by the MOLA (Mars Orbiter Laser Altimeter) instrument (Pettengill and Ford, 2000) in the same regions have been interpreted as signals returned by thick convective CO_2 ice clouds forming in the lowest 20 km (Colaprete and Toon, 2002; Tobie et al., 2003).

Other observations suggest CO_2 ice clouds could form at much higher altitudes. As recorded by Pathfinder during its descent in the equatorial region (Schofield et al., 1997) and other ground-based observations (Clancy and Sandor, 1998), CO_2 can exceed saturation conditions around 80 km. Spectroscopic evidence of atmospheric CO_2 ice was reported after the discovery of an emission spike at a wavelength of 4.3 μm from Mariner 6 and 7 infrared probings of the bright martian limb (Herr and Pimentel, 1970). Recent studies reveal in fact that this spectral feature was mistakenly confused with a resonant scattering band of CO_2 fluorescence (Drossart et al., 2005;

* Corresponding author. Fax: +33 (0) 1 69 20 29 99.
E-mail address: franck.montmessin@aero.jussieu.fr (F. Montmessin).

0019-1035/$ – see front matter
doi:10.1016/j.icarus.2006.03.015

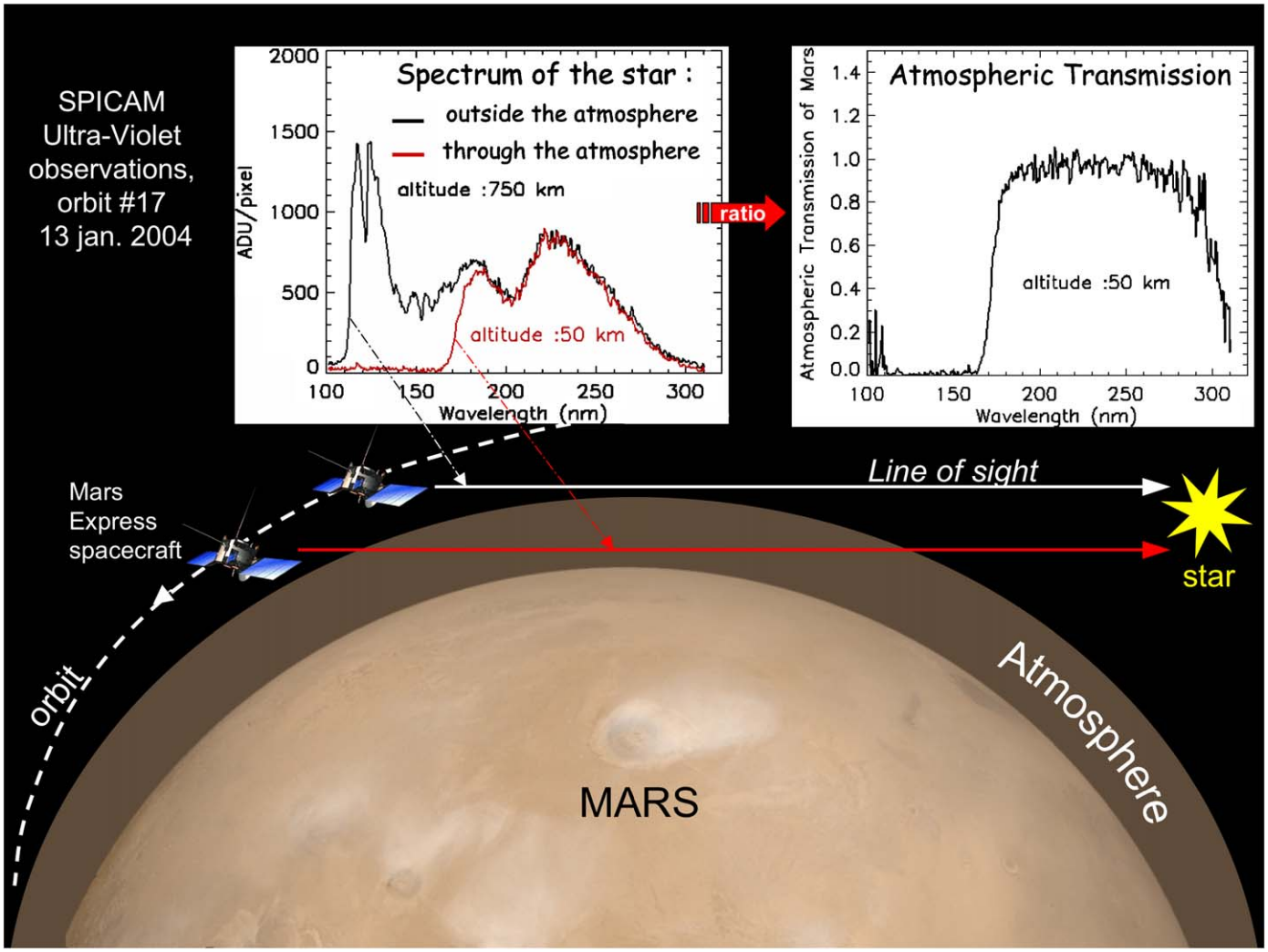

Fig. 1. Schematic sketch of an occultation. All along the orbit, Mars Express maintains a position allowing SPICAM to constantly image the star in the central band of the detector. SPICAM first collects a reference spectrum when it is far enough from the planet for the atmosphere to be considered transparent to the stellar illumination. As the spacecraft proceeds, its line of sight progressively penetrates deeper into the atmospheric shell and light gets extinguished by species present on the optical path. From the two spectra obtained outside and through the atmosphere, an atmospheric transmission can be derived. Displayed spectra come from the very first stellar occultation made by SPICAM at the beginning of the mission, which is also the very first made by any instrument orbiting around Mars. Shortward of 180 nm, the signal is completely attenuated by CO_2 absorption.

López-Valverde et al., 2005). Nonetheless, the notion that CO_2 ice clouds would frequently appear in the martian mesosphere was suggested on the basis of Mars Pathfinder images showing bright, bluish morning clouds (Smith et al., 1997) that Schofield et al. (1997) and Clancy and Sandor (1998) have suggested to result from supercold (supersaturated) atmospheric manifestations at high altitude.

2. Stellar occultation data

The SPICAM (SPectroscopy for the Investigation of the Characteristics of the Atmosphere of Mars) instrument on board Mars Express (MEx) is a UV-IR dual spectrometer dedicated primarily to the study of the atmosphere of Mars (Bertaux et al., 2000, 2005a, 2005b). The observations discussed here were made in the stellar occultation mode using the UV channel. These data show for the first time several occurrences of CO_2 ice clouds at the highest altitudes ever recorded for a cloud layer on Mars. The UV channel is a full imaging spectrometer which spans the 118–320 nm wavelength range with a resolution of 1.5 nm. Stellar occultations are performed when the whole Mars Express spacecraft orients itself to let SPICAM targeting a specific star on the night-side of the orbit. The star can be seen either rising or setting behind the horizon. Along the spacecraft trajectory, images of the star are collected both from outside and through the atmosphere and then ratioed to obtain the atmospheric transmission as a function of tangential altitude (a sketch of the observation geometry is shown in Fig. 1). By principle, these observations do not require a radiometric calibration of the instrument.

The whole UV data inversion method was originally developed for the ENVISAT mission in order to retrieve NO_x species and temperature profiles in the Earth atmosphere from stellar occultation data (Hauchecorne et al., 2005). The adaptation to Mars is described in details elsewhere (Quémerais et al., 2005). The 118–320 nm spectral range covered by the UV channel

bears the signature of CO_2, O_3 and aerosols (dust or/and cloud particles). Carbon dioxide and ozone have each a distinct absorption feature respectively shortward of 200 nm and around 250 nm (Yoshino et al., 1996; Parkinson et al., 2003). Aerosols contaminate the whole spectrum. We approximate their opacity as a function of wavelength using a formula commonly employed for terrestrial aerosols (Dubovik et al., 2000):

$$\tau_\lambda = \tau_{\lambda 0}(\lambda_0/\lambda)^\alpha$$

where λ is the wavelength in nanometers, $\tau_{\lambda 0}$ is the aerosol slant opacity at a reference wavelength λ_0 (taken here at 250 nm) and α is commonly referred as to the Angström coefficient. Larger α values are usually indicative of particles smaller than the sampled wavelength (Dubovik et al., 2000; O'Neill and Royer, 1993). Every spectrum is fitted using a Levenberg–Marquardt algorithm where CO_2 and O_3 amounts, as well as $\tau_{\lambda 0}$ and α are free parameters (see an example of fit in Fig. 2C). Instrumental noise causes a systematic uncertainty of about 5% in the retrieved quantities. The vertical profile of each species concentration is obtained with a standard "onion peeling" technique and a Tikhonov regularization to reduce numerical noise (Quémerais et al., 2005). Pressure profile is deduced from the vertical distribution of CO_2 density by integration of the hydrostatic equation. Temperature is then given by the ideal gas law. The altitude range of observations remains generally between 20 and 150 km. Above 150 km, atmospheric extinction is too weak to be detected at the 1-σ confidence level, whereas below 30 km, opacity of the martian haze becomes progressively so thick that SPICAM does not detect any photon. With a measurement frequency of 1 Hz, the vertical resolution usually ranges from 1 to 3 km.

To access the "true" wavelength dependence of aerosol extinction needed to estimate particle size, we first reconstruct synthetic transmissions by removing the pre-computed contributions of CO_2 and O_3 to the original spectra. It is then assumed that resulting transmissions are only shaped by the aerosol spectral behavior and an aerosol opacity is assigned to each pixel. The same vertical inversion as for the gaseous species is employed to deduce the vertical profile of aerosol extinction for each wavelength resolved by the instrument. Particle size is then deduced from a spectral fit performed between 200 and 280 nm at every altitude using Mie theory to reproduce extinction variation. Although sphericity is a poor approximation of the real shape of icy crystals, it only has minor effects on our conclusion. Our particle radius estimates are based on the measurement of the spectral slope of aerosol extinction, a forward scattering quantity almost independent of aerosol morphology (as recently reviewed by Wolff and Clancy, 2003). And while sophisticated methods exist (e.g., T-matrix) to compute scattering properties for nonspherical particles, their use is essentially justified when aerosols are observed at scattering angles $>40°$. Refractive indices were taken from several laboratory works (Warren, 1986) for CO_2 ice. Refractive indices of H_2O ice (Warren, 1984) and dust were also tested in order to assess how sensitive particle radius estimates are to the supposed composition. Optical properties of dust were taken from a compilation of orbiter observations (Ockert-Bell et al., 1997). These authors mention that results for dust in the UV cannot be reconciled with previous estimates and admit that dust spectral behavior remains problematic. However, it appears that the radius value is mildly sensitive to the supposed composition.

The 412 stellar occultations already performed by SPICAM cover a region extending between 75° S and 70° N and sample several seasons with L_s (the solar longitude, defined by the current position of Mars, that of the Sun and with the position of Mars at vernal equinox taken for reference) ranging from 330° (northern winter) to 200° (northern fall). Among this dataset, four profiles were found to exhibit the distinct presence of aerosol layers at more than 90 km (see Fig. 3 for the aerosol vertical profiles), an altitude much greater than the expected top of the dust layer at this season (Jaquin et al., 1986). Taking orbit 1226 as an example (the sequence of spectra is displayed in Fig. 2A), the presence of an isolated aerosol layer can be easily identified in the data as it creates a noticeable reduction of photon counts over the whole spectral range. The profile of atmospheric transmission shows a strong depression in the vicinity of the layer (Fig. 2B) near 100 km. Transmissions are affected everywhere between 200 and 280 nm (Fig. 2C), but are much more reduced at shorter wavelengths, the spectral signature of particles with sizes comparable or smaller than sampled wavelengths.

3. Interpretation

Simultaneous retrieval of the temperature profiles, displayed in Fig. 4, provides an important information helping to assess the nature of these clouds. Except in the case of orbit 1225, every profile exhibits a structure that was already noted in the temperature measurements of the ASI/MET experiment during Pathfinder descent through the martian atmosphere (Schofield et al., 1997): a strong heating occurs above 100 km due to CO_2 absorption of extreme ultraviolet, while temperatures reach a minimum between 90 and 110 km. The shape of the profile in that region, with a strong increase in the atmospheric lapse rate a few kilometers below the temperature minimum, suggests the cooling action of upward propagating thermal tides. The SPICAM profiles, ASI/MET data and other telescopic observations at submillimetric wavelengths (Clancy and Sandor, 1998) reveal that temperature can fall well below the CO_2 condensation point at high altitudes. The tops of the detached layers appear within (orbits 1209, 1225, and 1226) and very close (orbit 1205) these supercold pockets of air. The very high levels of supersaturation encountered there (down to 15 K below the condensation point, equivalent to saturation ratios of several tens) suggest that observed detached layers are probably mesospheric CO_2 ice clouds. Any particle flowing within such an environment is likely to nucleate and grow by deposition of CO_2 ice. A saturation excess of only 30% is typically required to initiate condensation (Glandorf et al., 2002) over a flat surface (note that greater supersaturation is needed when condensation occurs over a spherical substrate in order to overcome curvature effect). Dust and water ice make unlikely candidates: unreasonably high mass mixing ratios (thousands of ppms) would be required to match both cloud opacity and particle size. For wa-

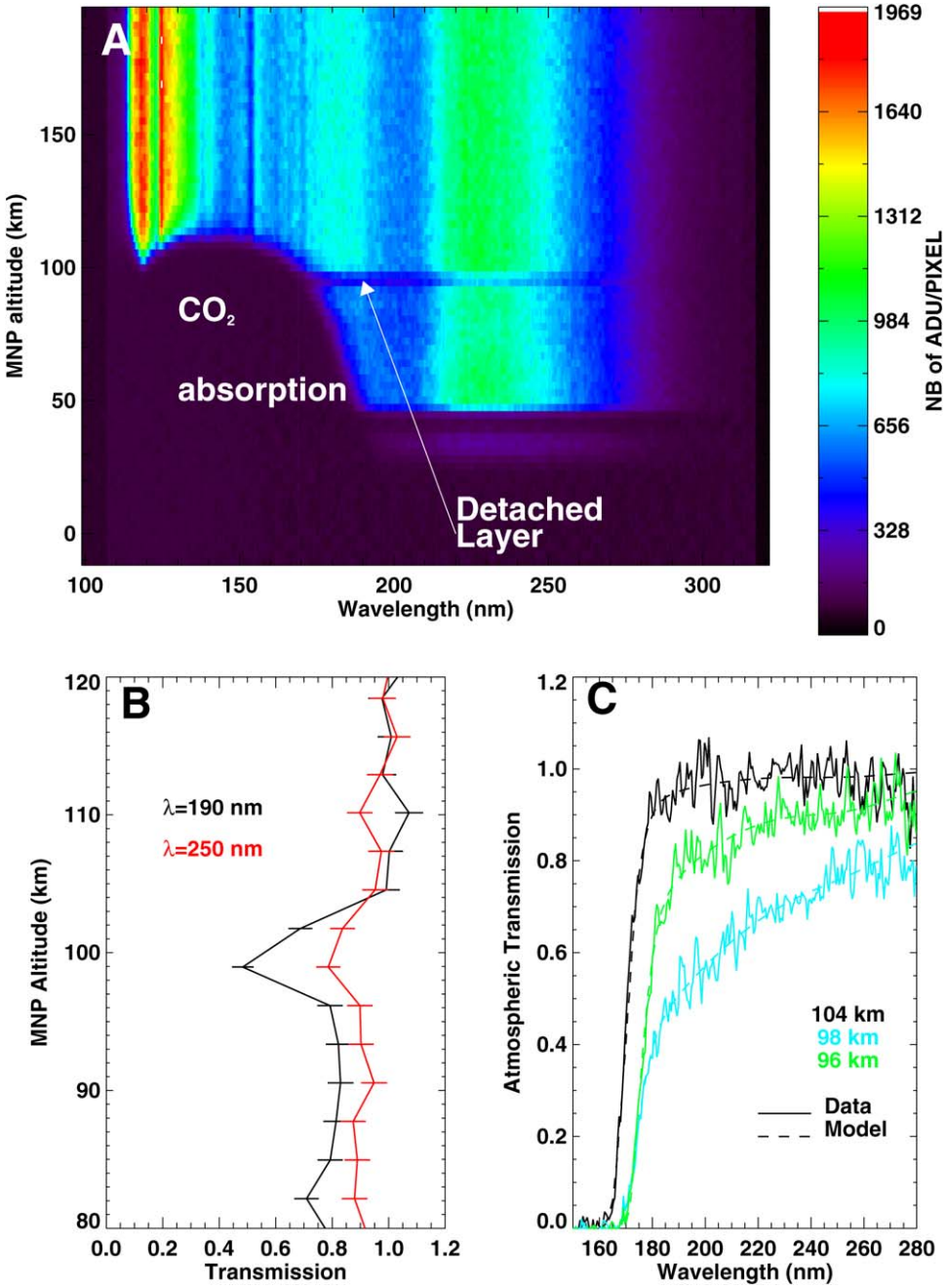

Fig. 2. (A) Sequence of star spectra obtained during occultation 1226A1. Raw intensity data are shown as Analog to Digital Unit (ADU—also known as Raw Detector counts) per pixel and have not been corrected for dark current. Data are projected on the altitude of the Mars nearest point (altitude above the point at which the line of sight is tangential to the atmospheric shell) defined above a reference ellipsoid. The CO_2 absorption feature shortward of 200 nm is recognizable, as is the presence of the detached layer which creates a general dimming over the CCD. (B) Data have been processed (dark current substraction) to yield the atmospheric transmission at various heights. Shown here are the profiles of transmission at two different wavelengths: 190 and 250 nm. Both transmissions decrease in the region of the detached layer around 100 km. The reduction of signal is however much more pronounced at 190 than at 250 nm. Error bars are also plotted on each profile. (C) Observed and modeled spectra at three altitudes in the region of the detached layer. The affect of the detached layer is present at every wavelength, as illustrated by the 98 km curve remaining systematically under the two others.

ter, such a concentration corresponds to its expected abundance at the surface of the north permanent cap when it sublimes in spring and summer, by far the wettest region observed on Mars.

Table 1 summarizes the main characteristics of the mesospheric clouds seen by SPICAM. These martian high altitude clouds match the description of terrestrial noctilucent clouds (NLC) which appear in the mesosphere of the polar regions (Reid et al., 1987; Thomas, 1991; Fiedler et al., 2003). Our inferred UV opacities ase typically very low (<0.01 when integrated over the vertical) and clouds would probably not be seen from the surface, unless perhaps after sunset or before sunrise when cloud particles can scatter sunlight coming directly from below the horizon. The blue morning clouds imaged by Pathfinder (Smith et al., 1997) possibly belong to the same class

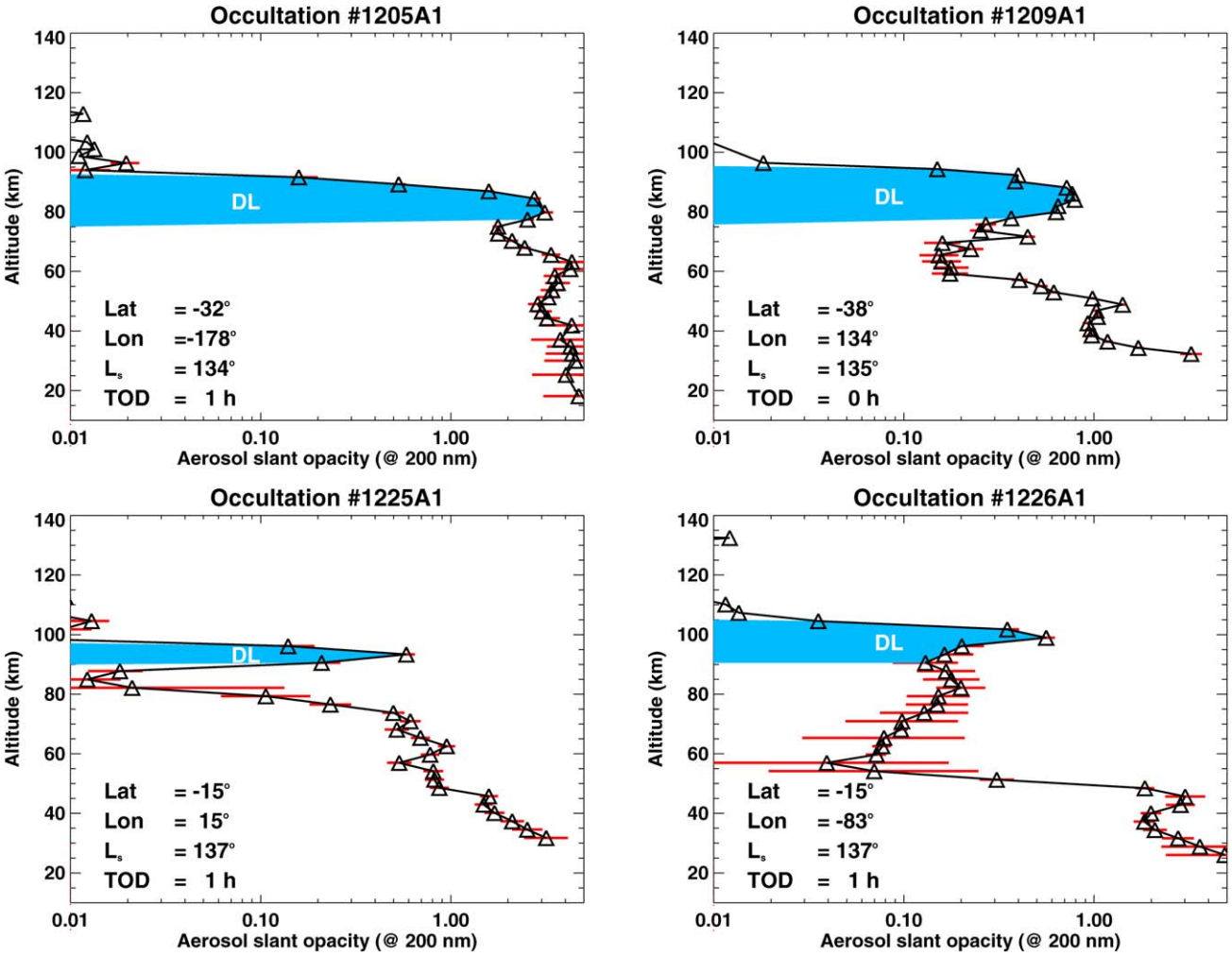

Fig. 3. Vertical profiles of the aerosol opacity (at 200 nm) along the line of sight for the 4 occultation sequences. The vertical extent of the detached layer (DL) is shown for reference but observation geometry may stretch the image of the layer to altitudes well below its actual lower limit. Locally, the layer is more confined vertically. All four occultations have been performed around midnight. Significant diurnal variations can be expected at high altitudes and clouds may disappear with daylight.

Table 1
List of the observation parameters for the four selected sequences of occultation discussed in the text

Orbit #	Date	Star name	L_s (°)	Lat (°)	Lon (°)	Local time	Z_{top} (km)	τ @ 200 nm	r_{eff} (nm)
1205	12/26/2004	Eps CMa	134	−32	−178	1:00 AM	92	0.05	110 ± 18
1209	12/27/2004	Als CMa	135	−36	134	12:00 AM	94	0.018	130 ± 12
1225	12/31/2004	Zet Pup	137	−15	15	1:00 AM	96	0.006	85 ± 18
1226	01/01/2005	Zet Pup	137	−15	−83	1:00 AM	101	0.008	80 ± 30

The four occultations occurred in a restricted period of time and in a restricted range of latitudes. Mesospheric clouds may appear more frequently than these data suggest, and SPICAM be only sensitive to the thickest ones. A value larger than 0.03 for the aerosol slant opacity is typically required to be detected at 1-σ level. This value was used to define the top (Z_{top}) of the detached layer. Cloud opacity (τ) is obtained by integration of the extinction profile over the vertical extent of the detached layer. Estimates of cloud particle sizes are made while assuming a pure CO_2 ice composition. The spectral behavior changes rapidly when particle size is of the same order of the wavelength, which makes our estimations particularly robust.

as the clouds presented here. When a pure CO_2 ice composition is assumed, cloud particle effective radius ranges between 80 and 130 nm. In comparison, NLC crystals on Earth rarely exceed 100 nm. At an altitude of 90–100 km, where the air density retrieved from the SPICAM data is only 0.1 mg m^{-3}, the fall velocity of 100 nm CO_2 particles exceeds 10 m s^{-1}. Despite the rapid fall of ice crystals, clouds might evolve in a steady-sate regime where the observed large amounts of supersaturated CO_2 allow a continuous condensation process and balance the mass lost by sedimentation. It is also possible that intense updrafts help maintain particles aloft or that martian mesospheric clouds are short-lived, explaining the few cases detected so far. It is indeed interesting to note that less than 1% of SPICAM occultations exhibit mesospheric ice clouds. This rate also reflects the frequency of supercold atmospheric manifestations appearing in the SPICAM data since the profiles discussed here

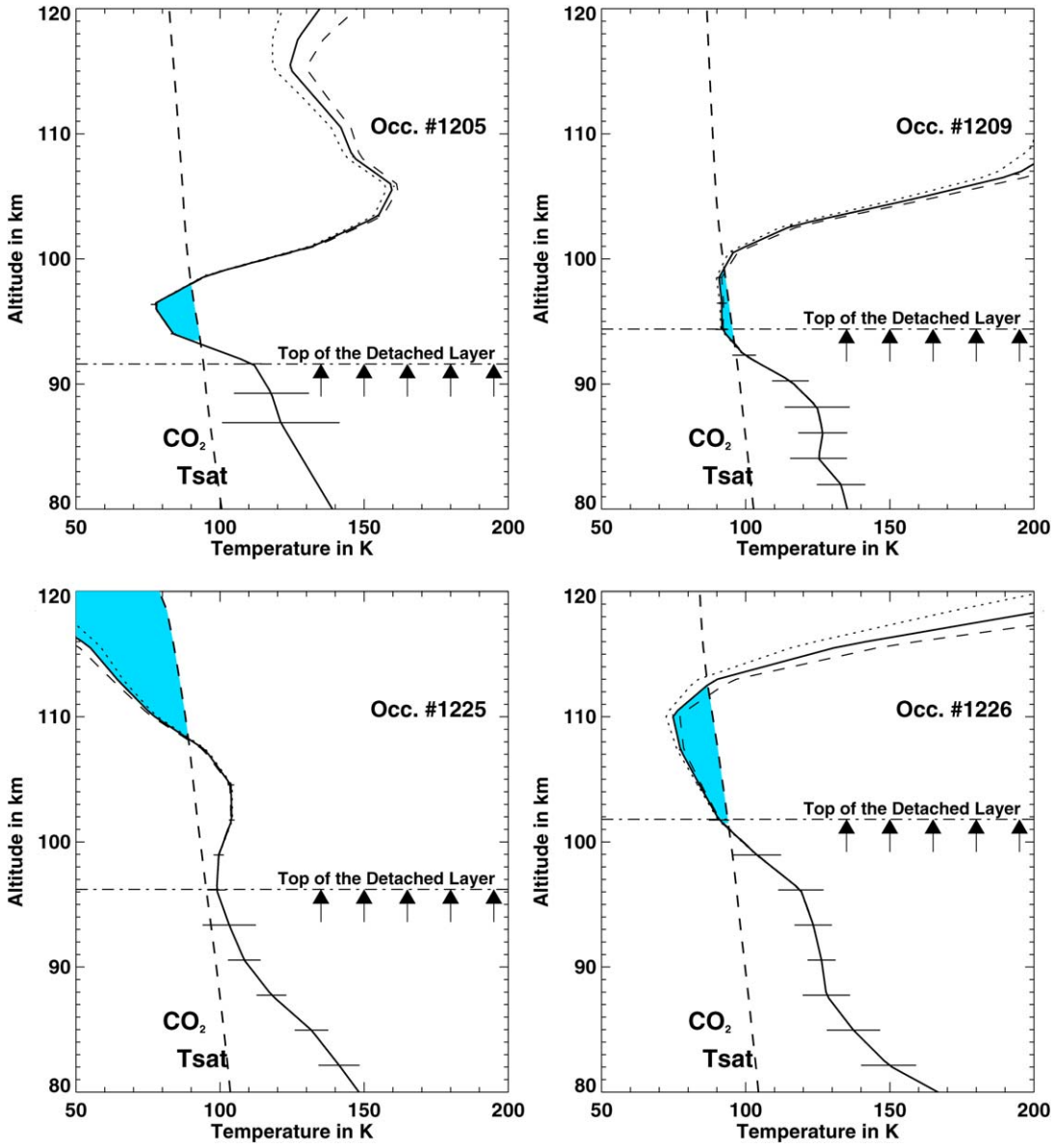

Fig. 4. Temperature profiles derived from the SPICAM occultation data. Dotted and dashed profiles show the envelope of uncertainty due to the temperature guess that must be made above the sounded region. A 3-σ uncertainty on temperature is represented by the small horizontal dashes intersecting thermal profiles. Shaded-blue portions represent zones where the atmosphere is supersaturated. The top of the detached layer appearing in the same observation sequence is shown for comparison. The slight offset between the cold pocket and the cloud top in orbit 1205 can be explained by CO_2 particles sedimenting out the supersaturated zone. A geometrical bias; i.e., a pronounced horizontal structure of the cloud cover, would also make the cloud appear lower than it actually is. Note also that vertical resolution is lower in that portion of the profile. Also, CO_2 cross-sections UV data used for the inversion are taken at only one temperature (195 K). No data is currently available for lower temperatures more representative of the martian atmosphere.

are the only one featuring a supersaturated portion of the atmosphere. This may result from SPICAM uneven sampling of the low latitude region where the action of vertically propagating thermal tides is expected to yield the strongest temperature amplitude variations (Zurek, 1976). We may then speculate that only because they are applied to the colder atmosphere of the near-aphelion season (during which the 100 km's detached layers have been inventoried), are diurnal tides able to cool CO_2 down to ice cloud formation.

Surprisingly, observed clouds systematically stretch below the supercold zone where they formed. A similar trend is observed for NLCs on Earth with respect to the saturation conditions of water vapor (Thomas, 1991). However, CO_2 ice particles can fall over significant distances into warmer, unsaturated air before their complete sublimation. In a rarefied atmosphere, condensation and sublimation processes are theoretically slower (Colaprete and Toon, 2003) and must therefore compete with the short timescales of sedimentation. Using our estimates on cloud opacity and particle size, we derive a cloud particle population of a few millions per cubic meter. Assuming CO_2 ice particles are formed heterogeneously, then a question stems about the origin of the cloud condensation nuclei. Could they be supplied by a flux of meteoritic debris like on Earth (Turco et al., 1982), or by an upward flux of

submicronic mineral dust particles stripped from the martian surface (Montmessin et al., 2002)? In any case, the presence of mesospheric clouds on Mars extends the atmospheric domain to be studied by scientists and addresses important questions about microphysical and dynamical properties of the upper martian atmosphere. Vertical propagation of waves appears only partly buffered by the release of latent heat induced by CO_2 condensation, as illustrated by the recurrent presence of supercold air pockets. In this context, the role played by microphysical processes, which control CO_2 ice particle formation and evolution, is critical in regulating the thermal state of the upper atmosphere and motivates the study of these "alien" clouds.

Acknowledgments

The authors thank two anonymous reviewers who have contributed significantly to improve this manuscript. Mars Express is a space mission from ESA (European Space Agency). We wish to express our gratitude to all ESA members who participated in this successful mission, and in particular to the ESOC team for the delicate controlling of the spacecraft, René Pischel and Tanja Zeghers at ESTEC for careful planning exercises. We thank also Astrium Corp. for the design and construction of the spacecraft, and in particular Alain Clochet. We thank our collaborators at the three institutes for the design and fabrication of the instrument (Service d'Aéronomie/France, BIRA/Belgium and IKI/Moscow), and in particular Emiel Van Raansbeck at BIRA for careful mechanical design. We wish to thank CNRS and CNES for financing SPICAM in France. We wish to thank the Space Division of the Belgian Federal Science Policy Office for supporting this project through the ESA PRODEX program. The Russian team acknowledges support of RFFI Grant 04-02-16856-a.

References

Bertaux, J.-L., Fonteyn, D., Korablev, O., Chassefière, E., Dimarellis, E., Dubois, J.P., Hauchecorne, A., Cabane, M., Rannou, P., Levasseur-Regourd, A.C., Cernogora, G., Quemerais, E., Hermans, C., Kockarts, G., Lippens, C., Maziere, M.D., Moreau, D., Muller, C., Neefs, B., Simon, P.C., Forget, F., Hourdin, F., Talagrand, O., Moroz, V.I., Rodin, A., Sandel, B., Stern, A., 2000. The study of the martian atmosphere from top to bottom with SPICAM light on Mars Express. Planet. Space Sci. 48, 1303–1320.

Bertaux, J., Leblanc, F., Perrier, S., Quemerais, E., Korablev, O., Dimarellis, E., Reberac, A., Forget, F., Simon, P.C., Stern, S.A., Sandel, B., 2005a. Nightglow in the upper atmosphere of Mars and implications for atmospheric transport. Science 307, 566–569.

Bertaux, J.L., Leblanc, F., Witasse, O., Quemerais, E., Lilensten, J., Stern, S.A., Sandel, B., Korablev, O., 2005b. Discovery of an aurora on Mars. Nature 435, 790–794.

Clancy, R.T., Sandor, B.J., 1998. CO_2 ice clouds in the upper atmosphere. Geophys. Res. Lett. 25, 489–492.

Colaprete, A., Toon, O.B., 2002. Carbon dioxide snow storms during the polar night on Mars. J. Geophys. Res. (Planets) 107, doi:10.1029/2001JE001758. 5-1.

Colaprete, A., Toon, O.B., 2003. Carbon dioxide clouds in an early dense martian atmosphere. J. Geophys. Res. (Planets) 108, doi:10.1029/2002JE001967. 6-1.

Drossart, P., and 9 colleagues, 2005. Non-LTE emission in atmospheric observations by OMEGA/Mars Express. In: Abstracts of the European Geophysical Union Conference in Vienna.

Dubovik, O., Smirnov, A., Holben, B.N., King, M.D., Kaufman, Y.J., Eck, T.F., Slutsker, I., 2000. Accuracy assessments of aerosol optical properties retrieved from Aerosol Robotic Network (AERONET) Sun and sky radiance measurements. J. Geophys. Res. 105 (14), 9791–9806.

Fiedler, J., Baumgarten, G., von Cossart, G., 2003. Noctilucent clouds above ALOMAR between 1997 and 2001: Occurrence and properties. J. Geophys. Res. 108 (D8), doi:10.1029/2002JD002419. 21.

Glandorf, D.L., Colaprete, A., Tolbert, M.A., Toon, O.B., 2002. CO_2 snow on Mars and early Earth: Experimental constraints. Icarus 160, 66–72.

Hauchecorne, A., Bertaux, J.-L., Dalaudier, F., Cot, C., Lebrun, J.-C., Bekki, S., Marchand, M., Kyrölä, E., Tamminen, J., Sofieva, V., Fussen, D., Vanhellemont, F., Fanton d'Andon, O., Barrot, G., Mangin, A., Théodore, B., Guirlet, M., Snoeij, P., Koopman, R., Saavedra de Miguel, L., Fraisse, R., Renard, J.-B., 2005. First simultaneous global measurements of nighttime stratospheric NO_2 and NO_3 observed by Global Ozone Monitoring by Occultation of Stars (GOMOS)/Envisat in 2003. J. Geophys. Res. 110 (D9). 18301.

Herr, K.C., Pimentel, G.C., 1970. Evidence for solid carbon dioxide in the upper atmosphere of Mars. Science 167, 47–49.

Hinson, D.P., Wilson, R.J., 2002. Transient eddies in the southern hemisphere of Mars. Geophys. Res. Lett. 29, doi:10.1029/2001GL014103. 58-1.

Jaquin, F., Gierasch, P., Kahn, R., 1986. The vertical structure of limb hazes in the martian atmosphere. Icarus 68, 442–461.

López-Valverde, M.A., López-Puertas, M., López-Moreno, J.J., Formisano, V., Grassi, D., Maturilli, A., Lellouch, E., Drossart, P., 2005. Analysis of CO_2 non-LTE emissions at 4.3 μm in the martian atmosphere as observed by PFS/Mars Express and SWS/ISO. Planet. Space Sci. 53, 1079–1087.

Montmessin, F., Rannou, P., Cabane, M., 2002. New insights into martian dust distribution and water-ice cloud microphysics. J. Geophys. Res. 107 (E6), doi:10.1029/2001JE001520.

Ockert-Bell, M.E., Bell, J.F., Pollack, J.B., McKay, C.P., Forget, F., 1997. Absorption and scattering properties of the martian dust in the solar wavelengths. J. Geophys. Res. 102 (E4), 9039–9050.

O'Neill, N., Royer, A., 1993. Extraction of bimodal aerosol-size distribution radii from spectral and angular slope (Angstrom) coefficients. Appl. Opt. 32, 1642–1645.

Parkinson, W.H., Rufus, J., Yoshino, K., 2003. Absolute cross section measurements of CO_2 in the wavelength region 163,200 nm and the temperature dependence. Chem. Phys. 219, 45–57.

Pettengill, G.H., Ford, P.G., 2000. Winter clouds over the north martian polar cap. Geophys. Res. Lett. 27, 609.

Quémerais, E., Bertaux, J.L., Korablev, O., Dimarellis, E., Cot, C., Sandel, B.R., Fussen, D., 2005. Stellar occultations observed by SPICAM on Mars Express, J. Geophys. Res. In press.

Reid, I.M., Ruester, R., Schmidt, G., 1987. VHF radar observations of cat's-eye-like structures at mesospheric heights. Nature 327, 43–45.

Schofield, J.T., Barnes, J.R., Crisp, D., Haberle, R.M., Larsen, S., Magalhaes, J.A., Murphy, J.R., Seiff, A., Wilson, G., 1997. The Mars Pathfinder Atmospheric Structure Investigation/Meteorology. Science 278, 1752–1758.

Smith, P.H., Bell, J.F., Bridges, N.T., Britt, D.T., Gaddis, L., Greeley, R., Keller, H.U., Herkenhoff, K.E., Jaumann, R., Johnson, J.R., Kirk, R.L., Lemmon, M., Maki, J.N., Malin, M.C., Murchie, S.L., Oberst, J., Parker, T.J., Reid, R.J., Sablotny, R., Soderblom, L.A., Stoker, C., Sullivan, R., Thomas, N., Tomasko, M.G., Ward, W., Wegryn, E., 1997. Results from the Mars Pathfinder Camera. Science 278, 1758–1765.

Thomas, G.E., 1991. Mesospheric clouds and the physics of the mesopause region. Rev. Geophys. 29, 553–575.

Tobie, G., Forget, F., Lott, F., 2003. Numerical simulation of the winter polar wave clouds observed by Mars Global Surveyor Mars Orbiter Laser Altimeter. Icarus 164, 33–49.

Turco, R.P., Toon, O.B., Whitten, R.C., Keesee, R.G., Hollenbach, D., 1982. Noctilucent clouds: Simulation studies of their genesis, properties and global influences. Planet. Space Sci. 30, 1147–1181.

Warren, S.G., 1984. Optical constants of ice from the ultraviolet to the microwave. Appl. Opt. 23, 1206–1225.

Warren, S.G., 1986. Optical constants of carbon dioxide ice. Appl. Opt. 25, 2650–2674.

Wolff, M.J., Clancy, R.T., 2003. Constraints on the size of martian aerosols

from Thermal Emission Spectrometer observations. J. Geophys. Res. 108 (E9), doi:10.1029/2003JE002057.

Yoshino, K., Esmond, J.R., Sun, Y., Parkinson, W.H., Ito, K., Matsui, T., 1996. Absorption cross section measurements of carbon dioxide in the wavelength region 118.7 nm–175.5 nm and the temperature dependence. J. Quant. Spectrosc. Rad. Transfer 50, 53–60.

Zurek, R.W., 1976. Diurnal tide in the martian atmosphere. J. Atmos. Sci. 33, 321–337.